

## Charge-Transfer Excited States in a $\pi$ -Stacked Adenine Dimer, As Predicted Using Long-Range-Corrected Time-Dependent Density Functional Theory

Adrian W. Lange, Mary A. Rohrdanz, and John M. Herbert\*

Department of Chemistry, The Ohio State University, Columbus, Ohio 43210

Received: March 8, 2008; Revised Manuscript Received: April 3, 2008

The lowest few electronic excitations of a  $\pi$ -stacked adenine dimer in its *B*-DNA geometry are investigated, in the gas phase and in a water cluster, using a long-range-corrected version of time-dependent density functional theory (TD-DFT) that asymptotically incorporates Hartree–Fock exchange. Long-range correction is shown to eliminate the catastrophic underestimation of charge-transfer (CT) excitation energies that plagues conventional TD-DFT, at the expense of introducing one adjustable parameter,  $\mu$ , that determines the length scale on which Hartree–Fock exchange is turned on. This parameter allows us to interpolate smoothly between hybrid density functionals and time-dependent Hartree–Fock theory. Excitation energies for CT states (in which an electron is transferred from one adenine molecule to the other) are found to increase dramatically as a function of  $\mu$ . Uncorrected hybrid functionals underestimate the CT excitation energies, placing them well below the valence excitations, while time-dependent Hartree–Fock calculations place these states well above the valence states. Values for  $\mu$  determined from certain benchmark calculations place the CT states well above the valence  $\pi\pi^*$  and  $n\pi^*$  states at the Franck–Condon point.

### I. Introduction

Half of a century ago, Eisinger concluded that the lowest excited states of oligonucleotides and DNA are excimer-like,<sup>1–3</sup> with relatively strong interactions between chromophores in the excited state, including some degree of charge transfer (CT) between nucleobases. Fifty years later, we are still debating the role of charge-transfer states in these systems. Much theoretical work on DNA employs so-called Frenkel exciton models,<sup>4–8</sup> in which CT is neglected and excited states consist exclusively of a linear combination of localized  $\pi \rightarrow \pi^*$  excitations. However, femtosecond transient absorption experiments<sup>9,10</sup> have revealed the existence of long-lived, optically dark “trap” states that are suggested to involve CT between nucleobases on the same DNA strand.<sup>10</sup>

Detailed quantum chemical calculations may ultimately shed light on this issue, but some problems must first be surmounted. One problem is system size; calculating excited states of a single purine base is already a taxing problem for correlated wave function methods. Although two- and three-base  $\pi$  stacks have been attacked with CASPT2 and CASSCF calculations, respectively,<sup>11,12</sup> serious compromises must be made regarding the choice of active space and basis set, and larger systems remain intractable. In contrast, the configuration interaction singles (CIS) method and time-dependent density functional theory (TD-DFT) can be applied to much larger systems, but already for  $\pi$ -stacked dimers, the predictions made by these methods are controversial. Low-lying CT states (<4 eV above the ground state) have been reported in two- and three-base  $\pi$  stacks on the basis of TD-DFT calculations,<sup>13,14</sup> but subsequent CIS and semiempirical ZINDO calculations failed to locate such

states,<sup>15,16</sup> and the TD-DFT results were thus ascribed to that method’s well-known proclivity toward severe underestimation of CT excitation energies.<sup>17–21</sup>

The appearance of intra- and intermolecular CT states, whose excitation energies may be underestimated by 10 eV or more, is a serious problem in small-molecule TD-DFT calculations but a catastrophic problem in larger systems,<sup>21–25</sup> where they ultimately form a near-continuum of spurious, optically dark excited states.<sup>21</sup> Thus, there are reasons to be suspicious of TD-DFT calculations in  $\pi$ -stacked nucleobase multimers (or hydrogen-bonded base pairs, for the same reason). Indeed, in one of the aforementioned TD-DFT studies of  $\pi$ -stacked dimers,<sup>14</sup> the authors mention the appearance of low-lying Rydberg states when diffuse basis functions are employed. Like CT states, Rydberg excitations are exquisitely sensitive to the asymptotic behavior of the exchange–correlation potential, and although Rydberg states may be unimportant in solution, their appearance at low excitation energies in the gas phase is a symptom of a deeper problem. Omission of diffuse basis functions pushes the Rydberg states to higher energies, concealing TD-DFT’s inherent inability to describe such states.

To correct TD-DFT’s shortcomings for Rydberg and CT states, several asymptotic corrections have been explored recently, each of which is based upon switching between a supposedly accurate (but asymptotically incorrect) exchange–correlation potential at short-range and an asymptotically correct (though not necessarily accurate) potential at long-range. The so-called statistical average of model orbital potentials<sup>26</sup> does this using two different “pure” (nonhybrid) potentials, and this method significantly improves the description of Rydberg states.<sup>26</sup> For CT states, nonlocal Hartree–Fock (HF) exchange is essential in the asymptotic limit,<sup>19</sup> and a different long-range-correction (LRC) technique has been investigated.<sup>27–31</sup> Within

\* To whom correspondence should be addressed. E-mail: herbert@chemistry.ohio-state.edu.

this approach, long-range HF exchange is grafted onto local (and therefore short-range) DFT, in an attempt to ameliorate the description of CT states without mucking up the delicate parametrization that yields high-quality results for properties that are insensitive to the tail of the exchange–correlation potential. This is accomplished by means of a switching function (typically the error function) applied to the Coulomb operator. The short-range part of the exchange interaction is then treated with local DFT and the long-range part with full HF exchange. This modification rectifies intermolecular CT energies, at least for well-separated monomers in the gas phase,<sup>32</sup> and is the correction scheme employed here.

In the present work, we apply the LRC to TD-DFT calculations of hydrated uracil clusters, a  $\pi$ -stacked adenine dimer in the gas phase, and the same  $\pi$ -stacked dimer in a water cluster. In a slight twist on previous tests of LRC-DFT, we employ a hybrid density functional, PBE0, since TD-PBE0 exhibits good accuracy for small, monomeric chromophores<sup>33</sup> and because a TD-PBE0 study of the  $\pi$ -stacked adenine dimer has recently appeared.<sup>34</sup>

## II. Theory and Methodology

We have implemented the LRC procedure described by Hirao and co-workers<sup>27,28</sup> for both pure and hybrid density functionals within a developers' version of Q-Chem.<sup>35</sup> The LRC consists of using the error function  $\text{erf}(\mu r)$ , where  $\mu$  is an adjustable parameter, to split the Coulomb operator into short- and long-range components

$$\frac{1}{r} = \frac{1 - \text{erf}(\mu r)}{r} + \frac{\text{erf}(\mu r)}{r} \quad (1)$$

The first term on the right decays to zero on a length scale of  $\sim 1/\mu$ , and the second term is a long-range background. Consider a density functional whose exchange–correlation energy can be written as

$$E_{xc} = E_c + (1 - C_{\text{HF}})E_{x,\text{local}} + C_{\text{HF}}E_{x,\text{HF}} \quad (2)$$

where  $C_{\text{HF}}$  represents the coefficient of HF exchange (e.g.,  $C_{\text{HF}} = 0.20$  for B3LYP and  $C_{\text{HF}} = 0.25$  for PBE0). Then, the LRC exchange–correlation energy for this functional is

$$E_{xc}^{\text{LRC}} = E_c + (1 - C_{\text{HF}})E_{x,\text{local}}^{\text{SR}} + C_{\text{HF}}E_{x,\text{HF}}^{\text{SR}} + E_{x,\text{HF}}^{\text{LR}} \quad (3)$$

where  $E_{x,\text{HF}}^{\text{SR}}$  and  $E_{x,\text{HF}}^{\text{LR}}$  denote the HF exchange energy evaluated using the short- and long-range parts of the Coulomb operator, respectively, and  $E_{x,\text{local}}^{\text{SR}}$  denotes the local exchange energy evaluated using the short-range part of the Coulomb operator. The correlation contribution  $E_c$  is not modified.

Exchange integrals over modified Coulomb operators, necessary to evaluate  $E_{x,\text{HF}}^{\text{SR}}$  and  $E_{x,\text{HF}}^{\text{LR}}$ , were implemented in Q-Chem by Gill and co-workers.<sup>36</sup> Short-range exchange is given by

$$E_{x,\text{local}}^{\text{SR}} = -\frac{1}{2} \sum_{\sigma} \int d\mathbf{r} \rho_{\sigma}^{4/3}(\mathbf{r}) K_{\sigma}^{\text{SR}}(\mathbf{r}) \quad (4)$$

where  $K_{\sigma}^{\text{SR}}$  is a short-range version of the exchange kernel  $K_{\sigma}$  for  $\sigma$  spin, which has a particular form for each generalized gradient approximation (GGA). Hirao and co-workers<sup>28</sup> provide a general prescription for obtaining  $K_{\sigma}^{\text{SR}}$  from  $K_{\sigma}$  for any GGA (see also ref 37).

We have implemented LRC versions of the Becke88 exchange<sup>38</sup> and the Perdew–Burke–Ernzerhof (PBE) exchange,<sup>39</sup> from which LRC variants of many common functionals can be constructed. We focus primarily on LRC-PBE0 in this work since the PBE0 functional has been recommended for its

**TABLE 1: Measures of CT Contamination in TD-DFT Calculations of (Uracil)(H<sub>2</sub>O)<sub>N</sub> (TDPBE0 data from ref 21)**

| <i>N</i> H <sub>2</sub> O | no. states below 6 eV |         | 40th excitation energy (eV) |         |
|---------------------------|-----------------------|---------|-----------------------------|---------|
|                           | PBE0                  | LRC-PBE | PBE0                        | LRC-PBE |
| 0                         | 5                     | 2       | 9.05                        | 10.60   |
| 4                         | 6                     | 2       | 8.06                        | 10.22   |
| 7                         | 11                    | 2       | 7.46                        | 9.80    |
| 15                        | 19                    | 2       | 6.60                        | 9.15    |
| 18                        | 20                    | 2       | 6.50                        | 8.95    |
| 25                        | 29                    | 2       | 6.22                        | 8.85    |
| 37                        | 59                    | 2       | 5.65                        |         |

accuracy in TD-DFT calculations<sup>33</sup> and has been used to study  $\pi$ -stacked dimers of 9-methyladenine, where low-energy CT states were reported.<sup>34</sup> All calculations discussed here utilize the 6-31+G\* basis set and the SG-1 quadrature grid.<sup>40</sup>

The TD-LRC-PBE0 method employed here has one adjustable parameter with two important limits: as  $\mu \rightarrow 0$ , the method reduces to TD-PBE0, and as  $\mu \rightarrow \infty$ , it reduces to time-dependent HF (TD-HF) theory, also known as the random-phase approximation. (The Tamm–Dancoff approximation is not made here, except in Table I in order to compare to results in ref 21.) In short, we have a method that can smoothly interpolate between two previous calculations, which reached opposite conclusions regarding the presence of low-energy CT states in  $\pi$ -stacked nucleobase dimers.

We consider three test systems: hydrated uracil clusters, taken from our previous work;<sup>21</sup> adenine dimer (A<sub>2</sub>) in its *B*-DNA geometry (3.4 Å separation and 36° twist angle), without phosphate or sugar moieties; and an A<sub>2</sub>(H<sub>2</sub>O)<sub>27</sub> cluster. In the latter, the water molecules were equilibrated by an aqueous-phase molecular dynamics simulation at  $T = 300$  K, constraining A<sub>2</sub> to retain its *B*-DNA geometry. All water molecules within 3 Å of A<sub>2</sub> were retained in the cluster. All geometries are available in the Supporting Information.

## III. Results

Standard TD-DFT calculations in large molecules and clusters are plagued by a high density of spurious CT excitations, not just at long-range but even at van der Waals contact distances.<sup>21</sup> We have investigated this problem previously using (uracil)(H<sub>2</sub>O)<sub>N</sub> clusters,<sup>21</sup> and in Table 1, we compare TD-PBE0 results from that study to TD-LRC-PBE results. The latter use  $\mu = 0.47 a_0^{-1}$  (where  $a_0^{-1}$  is the Bohr radius), a value recommended<sup>28</sup> for the LRC-BOP functional.<sup>41</sup> The LRC method predicts just two excited states below 6 eV (consistent with multireference calculations),<sup>42</sup> regardless of cluster size. Notably, when using a nonhybrid functional such as PBE, and absent any LRC, we were previously unable to perform TD-DFT calculations beyond  $N = 15$  due to the large number of states required to reach 6 eV.<sup>21</sup>

Turning now to the A<sub>2</sub> and A<sub>2</sub>(H<sub>2</sub>O)<sub>27</sub> calculations that are the main topics of this work, Figure 1 shows that TD-DFT vertical excitation energies for A<sub>2</sub> increasing monotonically as a function of  $\mu$ , consistent with the observation that the CIS and TD-HF methods ( $\mu = \infty$ ) tend to overestimate all excitation energies. For A<sub>2</sub>, the TD-HF method predicts only a few states within  $\sim 7$  eV of the ground state, but the density of states increases significantly as  $\mu \rightarrow 0$ .

By inspecting excited-state Mulliken charges, TD-DFT excitation amplitudes, natural transition orbitals,<sup>43</sup> and electron attachment/detachment densities,<sup>44</sup> we are able to construct diabatic states along which the excited states change smoothly as a function of  $\mu$ . Several such states are shown in Figure 2,

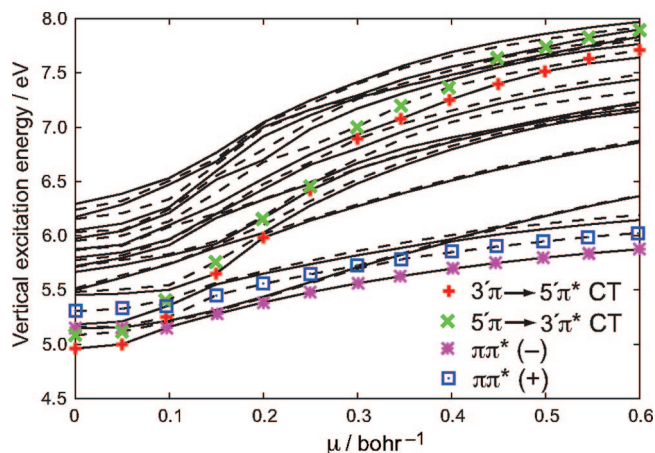


**Figure 1.** Vertical excitation energies for  $A_2$ , calculated at the TD-LRC-PBE0/6-31+G\* level as a function of the range-separation parameter  $\mu$ . The black lines are adiabatic excitation energies (alternating solid and broken, for clarity). The CT and  $\pi\pi^*$  diabatic states are also indicated (cf. Figure 2a).

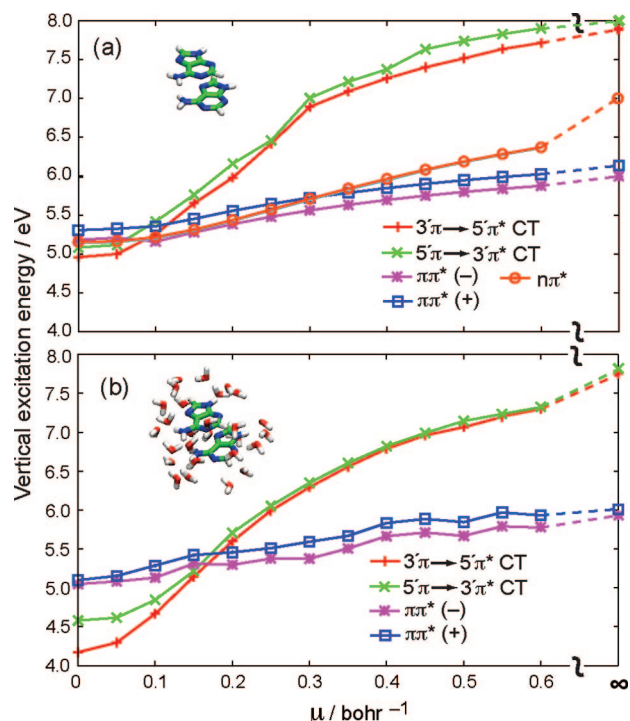


**Figure 2.** Diabatized vertical excitation energies as a function of the range-separation parameter  $\mu$  for (a) stacked adenine dimer,  $A_2$ , and (b)  $A_2(H_2O)_{27}$ . The two monomers are labeled 3' and 5', and the  $\pi\pi^*(-)$  and  $\pi\pi^*(+)$  labels indicate linear combinations of localized  $\pi \rightarrow \pi^*$  excitations ("Frenkel excitons"). Two  $n\pi^*$  states are plotted in (a), but they are indistinguishable on this scale.

including a pair of intermolecular CT states (one for each possible direction of intermolecular CT), a pair of Frenkel exciton states (plus/minus linear combinations of localized  $\pi \rightarrow \pi^*$  excitations), and a pair of localized  $n \rightarrow \pi^*$  states. The  $n\pi^*$  states, which are significantly blue-shifted by solvation, are not included for  $A_2(H_2O)_{27}$  due to the high cost of calculating enough excited states to reach them at small values of  $\mu$ . This difficulty is a direct consequence of the proliferation of low-lying excited states as  $\mu \rightarrow 0$ .

As expected, the CT states are far more sensitive to the value of  $\mu$  than are the valence states. (Rydberg states are also very sensitive to  $\mu$ , but these appear above the valence states of  $A_2$  at all values of  $\mu$ , even in the gas phase, and are thus omitted

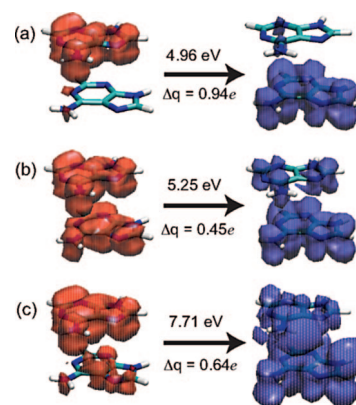


**Figure 3.** TD-LRC-PBE0 detachment and attachment densities for using (a)  $\mu = 0$ , (b)  $\mu = 0.10 a_0^{-1}$ , and (c)  $\mu = 0.6 a_0^{-1}$ . Each plot represents an isocontour that encompasses 70% of the total density. Also shown are the excitation energies and the amount of intermolecular CT ( $\Delta q$ ) upon excitation, as quantified by natural population analysis.

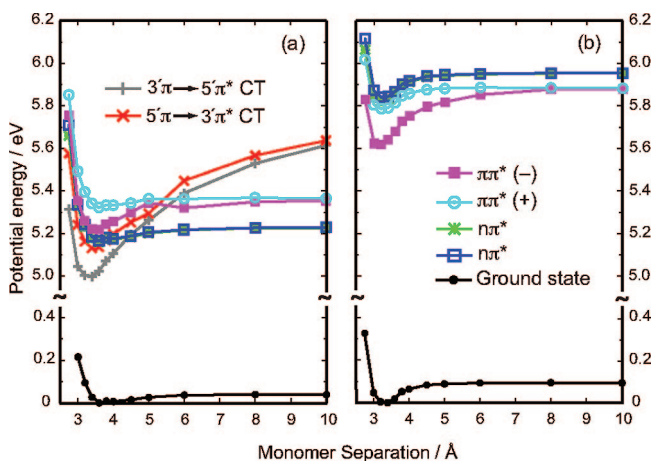


**Figure 4.** TD-LRC-PBE0 diabatic potential energy curves for  $A_2$  as a function of the intermolecular distance, using (a)  $\mu = 0$  and (b)  $\mu = 0.35 a_0^{-1}$ . The two  $n\pi^*$  potential curves overlap one another in both plots, and the CT states in (b) lie above 6.2 eV and are not shown.

from Figure 2a and from our discussion.) In the TD-PBE0 ( $\mu \rightarrow 0$ ) limit, the CT excitation energies appear at or below 5 eV and represent the lowest-energy excitations in both  $A_2$  and  $A_2(H_2O)_{27}$ . The water cluster stabilizes the CT states by  $\sim 0.5$  eV (roughly independent of  $\mu$ ) as compared to the gas phase; nevertheless, a TD-HF calculation ( $\mu = \infty$ ) places these states above 7 eV—too high to be biologically relevant at the Franck–Condon geometry. This is consistent with a previous CIS study of  $\pi$ -stacked dimers of nucleobases and base analogues, which reported no evidence of CT in the lowest few excited states.<sup>15</sup>

Figure 3 depicts electron attachment and detachment densities for the lower of the two CT states, at several values of  $\mu$ . For  $\mu = 0$ , this state corresponds to a net transfer of  $\Delta q = 0.94$  electrons between adenine molecules, as quantified by natural population analysis.<sup>45</sup> (Similar values of  $\Delta q$  are obtained from Mulliken population analysis.) The CT nature of this state is clearly evident at  $\mu = 0$ , but the character of this state is more mixed at larger values of  $\mu$ .

In Figure 4, we plot diabatic potential energy surfaces for gas-phase  $A_2$ , as a function of the monomer separation  $R$ , using  $\mu = 0$  and  $0.35 a_0^{-1}$ . (The diabats in Figure 2 correspond to vertical excitation at  $R = 3.4 \text{ \AA}$ .) For  $\mu = 0$  (TD-PBE0, Figure 4a), the  $S_1$  state is unambiguously a CT state at the Franck–

Condon point, while the  $S_1$  minimum appears at a smaller value of  $R$ —and is much deeper than—the shallow  $S_0$  minimum. These two features are the classic signatures of an excimer state, though we should note that both features are present also in the  $S_1$  state at  $\mu = 0.35 a_0^{-1}$  (Figure 4b), for which  $S_1$  is not a CT state but rather a  $\pi\pi^*$  state. This state appears at higher energy than does the lowest  $\pi\pi^*$  state for  $\mu = 0$  because the LRC has the effect of pushing all of the excited states to higher energy (albeit the CT states more so than the valence states). For reasons that we do not yet understand, the LRC also considerably deepens the ground-state minimum (which is too shallow at the PBE0 level due to lack of dispersion interactions) and also reduces the minimum-energy separation to 3.4 Å in the ground state.

#### IV. Discussion

Variation of  $C_{\text{HF}}$  in a standard (non-LRC) hybrid functional tends to shift all excitation energies upward as  $C_{\text{HF}}$  increases, at roughly the same rate (see the Supporting Information); the total shift from  $C_{\text{HF}} = 0$  to 1 is 2 eV or more for each excited state. This is to be contrasted with the variation of  $\mu$ , which affects the CT and Rydberg states to a much greater extent than the valence states since short-range exchange–correlation effects are largely preserved by the LRC but long-range exchange is fundamentally different. Furthermore, the character of the CT states changes as a function of  $\mu$ , as is evident from the attachment/detachment densities in Figure 3. For  $\mu \approx 0$ , the lowest CT state involves transfer of  $\approx 0.9$  electrons from the HOMO of the supersystem (which is localized on one adenine monomer) to the LUMO of the supersystem (localized on the other monomer), and this one excitation amplitude accounts for  $\sim 85\%$  of the norm of the TD-DFT eigenvector. However, starting at around  $\mu \approx 0.1 a_0^{-1}$  (where many of the adiabats in Figure 1 begin to shift rapidly as a function of  $\mu$ ), the character of this nominal CT state becomes more mixed, even while it continues to involve significant CT between the two adenine molecules. In the  $\mu \rightarrow \infty$  limit, no single excitation amplitude accounts for more than 12% of the norm of the TD-HF eigenvector.

Santoro et al.<sup>34</sup> have reported intermolecular CT states appearing just below 5 eV in a  $\pi$ -stacked dimer of 9-methyladenine using TD-PBE0 in conjunction with a polarizable continuum model of aqueous solvation. This calculation is comparable to our  $A_2(\text{H}_2\text{O})_{27}$  calculation with  $\mu = 0$ . Our results demonstrate that the solvent stabilization is only partially responsible for the low energy of the CT states. Certainly, the solvent does preferentially stabilize these states, relative to the valence states, but the more important factor in their appearance at low energies is the tuning of the range parameter  $\mu$ .

Thus, the crucial question is which  $\mu$  value to use. One could imagine adjusting  $\mu$  to reproduce high-level ab initio calculations for the gas-phase adenine monomer,<sup>46–48</sup> but in fact, there is considerable variation in these supposed benchmarks, and even the order of the states is sensitive to the level of theory.<sup>46</sup> Our  $\mu = 0$  value for the excitation energy to the lowest bright state (“ $L_a$ ”) is 5.3 eV at the  $B$ -DNA geometry (evident in the asymptote of Figure 4a) or 5.2 eV if the geometry is optimized with PBE0. These values fall within the 4.90–5.35 eV range of recent CASPT2 estimates.<sup>47,48</sup> MRCI calculations, however, place this state at least 5.7 eV above the ground state (and possibly higher),<sup>46</sup> and  $\mu = 0.35 a_0^{-1}$  or even larger would be consistent with such a value. All values of  $\mu$  in this range reproduce the 0.05 eV decrease in the  $L_a$  excitation energy that is observed upon  $\pi$  stacking.<sup>16</sup>

Several previous studies of LRC-DFT have optimized  $\mu$  using ground-state benchmarks including atomization energies and

barrier heights. For the LRC-BOP functional<sup>41</sup> (a reparameterization of LRC-BLYP) and the LRC- $\omega$ PBE functional<sup>49</sup> (a different formulation of LRC-PBE), these fits afford  $\mu = 0.47 a_0^{-1}$  and  $0.40 a_0^{-1}$ , respectively.<sup>28,49</sup> However, the statistically optimal value of  $\mu$  for ground-state properties may not be the best value for excitation energies; therefore, we have optimized  $\mu$  in LRC-PBE0 so as to reproduce the SAC-CI potential energy curve<sup>32</sup> for the lowest CT excitation in the  $\text{C}_2\text{H}_4\cdots\text{C}_2\text{F}_4$  heterodimer. (Energies and geometries from this calculation are available in the Supporting Information.) Even if the SAC-CI benchmarks are all shifted by  $\pm 0.2$  eV, this procedure affords optimal  $\mu$  values that lie between the two values suggested above. For  $\mu$  in this range, the CT states in  $A_2(\text{H}_2\text{O})_{27}$  lie more than 1 eV above the  $\pi\pi^*$  states, at least at the Franck–Condon point.

The present work makes clear that one must be extremely wary of TD-DFT predictions of intermolecular CT states, even at base-stacking distances. A more comprehensive study of this issue, including a simultaneous optimization of  $\mu$  against both ground- and excited-state benchmarks, is currently underway in our group.

**Acknowledgment.** This work was supported by a NSF CAREER award, by the ACS Petroleum Research Fund, and by start-up funds from The Ohio State University. Calculations were performed at the Ohio Supercomputer Center.

**Supporting Information Available:** Gas-phase geometries and excitation energies. This material is available free of charge via the Internet at <http://pubs.acs.org>.

#### References and Notes

- (1) Eisinger, J.; Guéron, M.; Shulman, R. G.; Yamane, T. *Proc. Natl. Acad. Sci. U.S.A.* **1966**, *55*, 1015.
- (2) Guéron, M.; Shulman, R. G.; Eisinger, J. *Proc. Natl. Acad. Sci. U.S.A.* **1966**, *56*, 814.
- (3) Eisinger, J.; Shulman, R. G. *Science* **1968**, *161*, 1311.
- (4) Bouvier, B.; Gustavsson, T.; Markovitsi, D.; Millié, P. *Chem. Phys.* **2002**, *275*, 75.
- (5) Bouvier, B.; Dognon, J.-P.; Lavery, R.; Markovitsi, D.; Millié, P.; Onidas, D.; Zakrzewska, K. *J. Phys. Chem. B* **2003**, *107*, 13512.
- (6) Emanuele, E.; Markovitsi, D.; Millié, P.; Zakrzewska, K. *ChemPhysChem* **2005**, *6*, 1387.
- (7) Bittner, E. R. *J. Chem. Phys.* **2006**, *125*, 094909.
- (8) Bittner, E. R. *J. Photochem. Photobiol., A* **2007**, *190*, 328.
- (9) Crespo-Hernández, C. E.; Kohler, B. *J. Phys. Chem. B* **2004**, *108*, 11182.
- (10) Crespo-Hernández, C. E.; Cohen, B.; Kohler, B. *Nature* **2005**, *436*, 1141.
- (11) Olasso-González, G.; Roca-Sanjuán, D.; Serrano-Andrés, L.; Merchán, M. *J. Chem. Phys.* **2006**, *125*, 231102.
- (12) Blancfort, L.; Voityuk, A. A. *J. Phys. Chem. A* **2006**, *110*, 6426.
- (13) Jean, J. M.; Hall, K. B. *Proc. Natl. Acad. Sci. U.S.A.* **2001**, *98*, 37.
- (14) Jean, J. M.; Hall, K. B. *Biochemistry* **2002**, *41*, 13152.
- (15) Hardman, S. J. O.; Thompson, K. C. *Biochemistry* **2006**, *45*, 9145.
- (16) Hu, L.; Zhao, Y.; Wang, F.; Chen, G.; Ma, C.; Kwok, W.-M.; Phillips, D. L. *J. Phys. Chem. B* **2007**, *111*, 11812.
- (17) Tozer, D. J.; Amos, R. D.; Handy, N. C.; Roos, B. O.; Serrano-Andrés, L. *Mol. Phys.* **1999**, *97*, 859.
- (18) Tozer, D. J. *J. Chem. Phys.* **2003**, *119*, 12697.
- (19) Dreuw, A.; Weisman, J. L.; Head-Gordon, M. *J. Chem. Phys.* **2003**, *119*, 2943.
- (20) Dreuw, A.; Head-Gordon, M. *J. Am. Chem. Soc.* **2004**, *126*, 4007.
- (21) Lange, A.; Herbert, J. M. *J. Chem. Theory Comput.* **2007**, *3*, 1680.
- (22) Bernasconi, L.; Sprik, M.; Hutter, J. *J. Chem. Phys.* **2003**, *119*, 12417.
- (23) Bernasconi, L.; Sprik, M.; Hutter, J. *Chem. Phys. Lett.* **2004**, *394*, 141.
- (24) Neugebauer, J.; Louwse, M. J.; Baerends, E. J.; Wesolowski, T. A. *J. Chem. Phys.* **2005**, *122*, 094115.
- (25) Neugebauer, J.; Gritsenko, O.; Baerends, E. J. *J. Chem. Phys.* **2006**, *124*, 214102.
- (26) Schipper, P. R. T.; Gritsenko, O. V.; van Gisbergen, S. J. A.; Baerends, E. J. *J. Chem. Phys.* **2000**, *112*, 1344.

- (27) Iikura, H.; Tsuneda, T.; Yanai, T.; Hirao, K. *J. Chem. Phys.* **2001**, *115*, 3540.
- (28) Song, J.-W.; Hirose, T.; Tsuneda, T.; Hirao, K. *J. Chem. Phys.* **2007**, *126*, 154105.
- (29) Yanai, T.; Tew, D. P.; Handy, N. C. *Chem. Phys. Lett.* **2004**, *393*, 51.
- (30) Vydrov, O. A.; Scuseria, G. E. *J. Chem. Phys.* **2006**, *125*, 234109.
- (31) Chai, J.-D.; Head-Gordon, M. *J. Chem. Phys.* **2008**, *128*, 084106.
- (32) Tawada, Y.; Tsuneda, T.; Yanagisawa, S.; Yanai, T.; Hirao, K. *J. Chem. Phys.* **2004**, *120*, 8425.
- (33) Adamo, C.; Scuseria, G. E.; Barone, V. *J. Chem. Phys.* **1999**, *111*, 2889.
- (34) Santoro, F.; Barone, V.; Imbrota, R. *Proc. Natl. Acad. Sci. U.S.A.* **2007**, *104*, 9931.
- (35) Shao, Y.; Fusti-Molnar, L.; Jung, Y.; Kussmann, J.; Ochsenfeld, C.; Brown, S. T.; Gilbert, A. T. B.; Slipchenko, L. V.; Levchenko, S. V.; O'Neill, D. P., Jr.; Lochan, R. C.; Wang, T.; Beran, G. J. O.; Besley, N. A.; Herbert, J. M.; Lin, C. Y.; Van Voorhis, T.; Chien, S. H.; Sodt, A.; Steele, R. P.; Rassolov, V. A.; Maslen, P. E.; Korambath, P. P.; Adamson, R. D.; Austin, B.; Baker, J.; Byrd, E. F. C.; Dachsel, H.; Doerksen, R. J.; Dreuw, A.; Dunietz, B. D.; Dutoi, A. D.; Furlani, T. R.; Gwaltney, S. R.; Heyden, A.; Hirata, S.; Hsu, C.-P.; Kedziora, G.; Khalliulin, R. Z.; Klunzinger, P.; Lee, A. M.; Lee, M. S.; Liang, W.; Lotan, I.; Nair, N.; Peters, B.; Proynov, E. I.; Pieniazek, P. A.; Rhee, Y. M.; Ritchie, J.; Rosta, E.; Sherrill, C. D.; Simmonett, A. C.; Subotnik, J. E.; Woodcock, H. L., III; Zhang, W.; Bell, A. T.; Chakraborty, A. K.; Chipman, D. M.; Keil, F. J.; Warshel, A.; Hehre, W. J.; Schaefer, H. F., III; Kong, J.; Krylov, A. I.; Gill, P. M. W.; Head-Gordon, M. *Phys. Chem. Chem. Phys.* **2006**, *8*, 3172.
- (36) Adamson, R. D.; Dombroski, J. P.; Gill, P. M. W. *J. Comput. Chem.* **1999**, *20*, 921.
- (37) Gill, P. M. W.; Adamson, R. D.; Pople, J. A. *Mol. Phys.* **1996**, *88*, 1005.
- (38) Becke, A. D. *Phys. Rev. A* **1988**, *38*, 3098.
- (39) Perdew, J. P.; Burke, K.; Ernzerhof, M. *Phys. Rev. Lett.* **1996**, *77*, 3865.
- (40) Gill, P. M. W.; Johnson, B. G.; Pople, J. A. *Chem. Phys. Lett.* **1993**, *209*, 506.
- (41) Tsuneda, T.; Suzumura, T.; Hirao, K. *J. Chem. Phys.* **1999**, *110*, 10664.
- (42) Lorentzon, J.; Fülcher, M. P.; Roos, B. O. *J. Am. Chem. Soc.* **1995**, *117*, 9265.
- (43) Martin, R. L. *J. Chem. Phys.* **2003**, *118*, 4775.
- (44) Head-Gordon, M.; Grana, A. M.; Maurice, D.; White, C. A. *J. Phys. Chem.* **1995**, *99*, 14261.
- (45) Reed, A. E.; Weinstock, R. B.; Weinhold, F. *J. Chem. Phys.* **1985**, *83*, 735.
- (46) Matsika, S. *J. Phys. Chem. A* **2005**, *109*, 7538.
- (47) Perun, S.; Sobolewski, A. L.; Domcke, W. *J. Am. Chem. Soc.* **2005**, *127*, 6257.
- (48) Serrano-Andrés, L.; Merchán, M.; Borin, A. C. *Chem.—Eur. J.* **2006**, *12*, 6559.
- (49) Vydrov, O. A.; Heyd, J.; Krukau, A. V.; Scuseria, G. E. *J. Chem. Phys.* **2006**, *125*, 074106.

JP802058K

ADDITIONS AND CORRECTIONS

---

2008, Volume 112B

**Adrian W. Lange, Mary A. Rohrdanz, and John M. Herbert\*:**  
Charge-Transfer Excited States in a  $\pi$ -Stacked Adenine Dimer,  
As Predicted Using Long-Range-Corrected Time-Dependent  
Density Functional Theory

Pages 6304–6308. In our recent Letter concerning long-range-corrected (LRC) time-dependent density functional theory (TD-DFT), we erroneously stated that the TD-LRC-DFT method reduces to time-dependent Hartree–Fock theory in the limit that the range separation parameter,  $\mu$ , tends to infinity. In fact, the  $\mu \rightarrow \infty$  limit corresponds to an exchange–correlation functional of the form  $E_{xc} = E_c + E_x^{\text{HF}}$ , where  $E_c$  is the DFT correlation energy and  $E_x^{\text{HF}}$  is the Hartree–Fock exchange energy. In other words, between  $\mu = 0$  and  $\infty$ , the TD-LRC-DFT method interpolates between some standard exchange–correlation functional ( $\mu = 0$ ) and a new functional, in which all local exchange has been completely replaced by nonlocal Hartree–Fock exchange ( $\mu = \infty$ ). The data, and thus the conclusions reached in our Letter, are unaffected by this error.

10.1021/jp803803j

Published on Web 05/21/2008